In situ biostimulation of Cr(VI) reduction in a fast-flowing oxic aquifer

Tatiana Nazarova[a,b], *Daniel S. Alessi*[c,d], *David J. Janssen*[a], *Rizlan Bernier-Latmani*[d], *Christoph Wanner*[a,*]

[a]Institute of Geological Sciences, University of Bern, Baltzerstr. 1-3, CH-3012 Bern, Switzerland

[b]Swiss Federal Institute for Forest, Snow and Landscape Research (WSL), 8903 Birmensdorf, Switzerland

[c]Department of Earth and Atmospheric Sciences, University of Alberta, Edmonton, T6G 2E3, Canada

[d]Environmental Microbiology Laboratory, Environmental Engineering Institute, School of Architecture, Civil and Environmental Engineering, Ecole Polytechnique Fédérale de Lausanne, 1015 Lausanne, Switzerland

*Corresponding author (email: wanner@geo.unibe.ch, phone: +41316314023

KEYWORDS

Bioremediation

Molasses

Cr reduction

Cr isotopes

Preferential flow paths

Column experiment

ABSTRACT

Hexavalent chromium is among the most common and hazardous inorganic contaminants in soils and groundwater. A promising *in situ* bioremediation approach is the delivery of electron donors to stimulate microbially-mediated Cr(VI) reduction, producing relatively insoluble Cr(III) precipitates. Even though this strategy has been implemented successfully in the past, it was primarily under favorable hydrological conditions, such as relatively slow groundwater flow velocities. To evaluate whether microbially-mediated Cr(VI) reduction can be sustained at high groundwater flow velocities and nearly oxygen-saturated conditions, we have conducted laboratory-scale column experiments and a field-scale pilot study using molasses as the electron donor. Despite the unfavorable conditions, both experiments provided clear evidence for microbially-mediated Cr(VI) reduction. In particular, the well used for injection in the field experiment became anoxic after two months of injection and the Cr(VI) concentration decreased by a factor of six. After stopping the injection, these conditions prevailed for at least four months. In the column experiments, Cr(VI)

reduction was accompanied by distinct Cr isotopic fractionation characterized by an enrichment factor of -1.25‰. In contrast, Cr isotope data collected from the field experiment were ambiguous, which was due to the complexation of Cr(III) with organic carbon and the heterogeneous distribution of molasses due to the presence of narrow preferential flow paths. A substantial injectivity decrease likely caused by the formation of biofilm and the precipitation of Fe-sulfides formed an additional challenge during the field experiment. Our data, however, also suggest that most of the identified challenges could be addressed by limiting the targeted dissolved organic carbon concentrations to about 10 mg/L. In conclusion, the injection of molasses constitutes a promising bioremediation strategy for the long-term treatment of Cr(VI) contamination even at high flow rates and under oxic conditions.

INTRODUCTION

Chromium is a heavy metal with two stable oxidation states. Trivalent chromium Cr(III) is the most common naturally occurring state.[1] At *pH* conditions commonly found in surface and groundwater (*pH* 6–9), Cr(III) has a very limited solubility and either adsorbs on solid particles or co-precipitates with Fe(III) hydroxides.[2] In contrast, hexavalent chromium, Cr(VI), is of primarily anthropogenic origin. It has numerous industrial applications including metal processing, leather tanning or wood preservation, and is therefore frequently found as a pollutant at industrial sites. Cr(VI) has mutagenic and carcinogenic effects on humans and animals, and prolonged exposure may cause birth defects and affect reproductive health.[3] Unlike Cr(III), Cr(VI) is highly soluble and likely to spread in surface water and groundwater. The thermodynamic stability of Cr(III) and of Cr(VI) in aqueous solutions depends on the *pH* and redox conditions of the system. Cr(VI) species (e.g., CrO_4^{2-}, $HCrO_4^-$, $Cr_2O_7^{2-}$)

are stable at oxidizing conditions, whereas species of Cr(III) (e.g., Cr^{3+}, $Cr(OH)^{2+}$, $Cr(OH)_2^+$, $Cr(OH)_3$, and $Cr(OH)_4$) occur under reducing conditions.

Due to its toxicity and high mobility, Cr(VI) represents a serious threat to the environment. Its impact, however, can be greatly decreased by its reduction to less toxic Cr(III).[4] Because the oxidation reaction with O_2 is kinetically inhibited, Cr(III) is stable in most natural surface environments even at oxidizing conditions that thermodynamically favor Cr(VI).[1,5] Aquifers containing manganese oxides represent the only exception, as these can oxidize Cr(III) much more rapidly.[1,6] Therefore, in the absence of manganese oxides, the reduction of Cr(VI) to Cr(III) is a durable and sustainable Cr immobilization method.

Some bacteria are capable of direct metabolic reduction of Cr(VI) by using Cr(VI) as a terminal electron acceptor.[7-9] However, the ability of bacteria to reduce Cr(VI) does not necessarily translate to a significant effect on chromate in contaminated environments, because the rate of conversion of Cr(VI) to Cr(III) by metabolic processes alone might be slow.[10] In anoxic conditions, indirect biological processes dominate Cr(VI) reduction[10] and yield reduction rates high enough to represent an efficient remediation measure. In such cases, the microbial reduction of common terminal electron acceptors (e.g., O_2, Fe(III), or SO_4^{2-}) leads to the establishment of reduced conditions favorable to abiotic Cr(VI) reduction.[11,12] The successful use of electron donors such as lactate or molasses to stimulate microbially-mediated Cr(VI) reduction in both laboratory and field studies has been reported.[5,7,11-17] With the exception of bioremediation attempts carried out in the oxidizing alluvial aquifer along the Columbia River at Hanford in Washington State, USA,[5,14] these studies were mostly performed at nearly anoxic conditions. Thus, a large uncertainty remains for assessing the implementation of microbially-mediated Cr(VI) reduction as a cost-

effective and sustainable remediation method at high groundwater flow rates and under oxidizing conditions.

In this study, we present results from laboratory-scale column experiments and a small field-scale pilot study where molasses solutions were used to stimulate microbially-mediated Cr(VI) reduction at high flow velocities and nearly oxygen-saturated conditions in alluvial sediments. Our objectives were to (i) evaluate whether Cr(VI) reduction could be achieved under such conditions, (ii) quantify the extent of this reduction in the contamination plume, and (iii) identify the main challenges to be addressed for a site-scale implementation. To this end, we used a combination of traditional geochemical techniques (i.e., concentration measurements) and Cr isotope analyses, which allow to distinguish between reduction and dilution as potential causes for decreasing Cr concentrations.[13,18-20]

MATERIALS AND METHODS

Site description. The pilot study was carried out at the former Metallwerke Selve & Co. factory in Thun, Switzerland (Fig. 1), where chromic acid was routinely used until the mid-1970s for acid cleaning of copper wires. Occasional spillage of the acid led to its infiltration into the underlying carbonate-dominated alluvial gravel aquifer. Dissolution and cementation caused the formation of an "industrial rock" containing 2 wt.% Cr(VI), 50 wt.% Cu and 1 wt.% Zn.[21] The resulting contamination hotspot has a surface area of about 30 m^2 and a vertical extent up to 7 m.[19] Neither Cu nor Zn is detected in elevated concentrations in the groundwater. Hexavalent chromium, on the other hand, is readily mobilized and forms a contamination plume with concentrations up to 4 mg/L Cr(VI) in the vicinity of the hotspot, which corresponds to a 400-fold violation of the Swiss regulatory limit (10 μg/L).

The local groundwater flow regime is influenced by the seasonal evolution of the nearby Aare river and a hydroelectrical power station 250 m downstream of the hotspot (Fig. 1). Due to the hydraulic gradient induced by the station, the oxygen-saturated river water infiltrates into the aquifer upstream, flows through the Cr(VI) hotspot, and then recharges the depleted river downstream, resulting in groundwater flow rates up to 15 m/day.[19] These site-specific conditions lead to the presence of a 250 m long contamination plume with a high Cr(VI) concentration, in a fully oxidized, and slightly alkaline aquifer with a *pH* value of about 8.

The contamination hotspot cannot be excavated, as it lies beneath a protected historical building. In 2008, a permeable reactive barrier (PRB) filled with zero-valent iron shavings was constructed downstream from the hotspot in order to reduce the extent of the plume. However, the subsequent monitoring of the site, as well as multi-tracer experiments and Cr isotope analyses, demonstrated that most of the Cr(VI) flows around the barrier and is therefore not treated.[19] Thus, the site is still classified as a contaminated site requiring remediation.

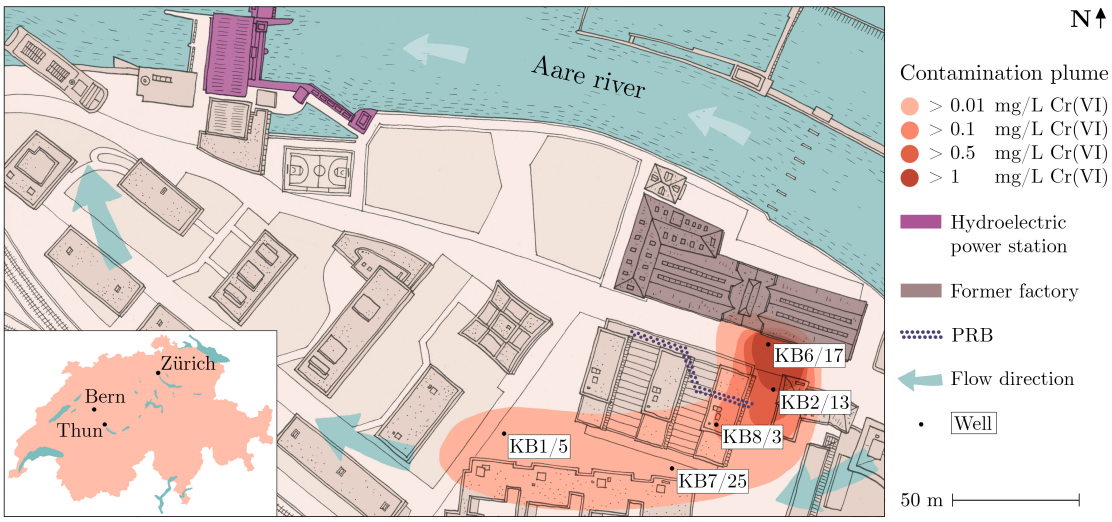

Figure 1. Schematic representation of the study site in Thun, Switzerland, showing the Cr(VI) contamination plume, the former building of the Metallwerke Selve & Co

factory, the hydroelectric power station, the PRB and the wells used for the field experiment.

Experimental approach. *Column experiments*. Two column experiments were performed to assess in a well-controlled setting whether microbially-mediated Cr(VI) reduction can be achieved under the oxic conditions and high flow rates specific to the site. Both experiments were run in a temperature-controlled room set to 20 °C to simulate summer conditions at the field site in Thun. Except for maintenance and sampling, the experiments were run in complete darkness. Both glass columns used (Kimble-Chase Kontes Chromaflex) had a length of 36.5 cm and an inner diameter of 3.5 cm, and were sterilized prior to being packed with Cr-free sediments. The porosities, measured gravimetrically, were 0.31 and 0.23. The sediments were collected on-site in October 2011 from a fresh basement excavation, 3 m below the ground surface and 200 m west of the contamination hotspot. They consisted of well-rounded coarse and pebble-sized grains dominated by quartz, clay minerals and calcite. After collection, the sediments were sieved in an Ar-filled glove bag to less than 2 mm within 24 hours and conserved in hermetically sealed Mylar bags in a freezer at EPFL at -80 °C until their use in the column experiment. The stock molasses used for the experiments was purchased from Schweizer Zucker AG. Its chemical composition is listed in Table 1.

Both columns were first covered in aluminum foil to block light and then flushed with deionized water for one week using a peristaltic pump (Ismatec IP ISM943) to achieve complete saturation. During the second week, Cr(VI)-contaminated groundwater collected from well KB2/13 (Fig. 1) was injected without addition of nutrients. The Cr(VI) concentration of the groundwater injected over the course of the experiment ranged from 0.39 to 0.63 mg/L, which is consistent with the concentration

range immediately downstream of the Cr(VI) hotspot (Fig. 1). The injection rate was set to a constant value of 2.05 mL/min, resulting in a residence time of 53 min for the first column and 39 min for the second column. The flow rates thus obtained were 10 and 13.5 m/day, respectively, which is consistent with field-site conditions.[19] From the third week onwards, a sterile molasses solution was injected through a second inlet (see Fig. S1, Supporting Information) at a flow rate of 0.1 mL/min to reach a low target molasses concentration of 200 mg/L. The target concentration is based on preliminary column experiments using the same Cr-free sediments[22] and was meant to minimize microbial overgrowth and possible clogging by biofilms. To equalize pressure, air was allowed to enter the molasses bottles through a vent protected by a 0.22 μm filter. Biofilm frequently developed in the molasses and groundwater feeding tubes despite the sterilization, and tended to decrease the flow rate and facilitate the disconnection of the tubes. This issue was addressed by frequent tubing changes.

Table 1: Composition of the stock molasses used in the field and laboratory experiments.

Compound	Concentration (wt. %)
Water content	28.1
Total dry matter	71.9
Total sugar	47.7
Other dry matter	24.2
Sucrose	43.9
Fructose	3.7
Glucose	< 0.5
Lactose	< 0.5
Maltose	< 0.5
Calcium	0.013
Phosphorus	0.174
Magnesium	0.192
Potassium	3.654
Sodium	0.521

Field experiment. Roughly 100 kg of molasses was injected into well KB6/17 (Fig. 1) between May 30 and September 29, 2018 using an Ismatec IPC peristaltic pump. To this end, concentrated stock molasses purchased from Schweizer Zucker AG (Table 1) was diluted with deionized water in 10 L heat-resistant polypropylene canisters and sterilized in an autoclave at 121 °C. The lids of the canisters were pierced to accommodate an outflow tube and sealed with Parafilm prior to autoclaving in order to minimize exchange with the outside air. Once a week, the canisters were replaced, and the injection tubes were cleaned with deionized water and alcohol. The equipment was stored on the sidewalk in a 1.8 m long, 0.65 m wide, and 0.6–0.7 m high wooden garden box with an aluminum covered lid (see Fig. S2,

Supporting Information). A hole was placed at the bottom of the box to allow access to the injection well.

The injection well KB6/17 is screened between 7 and 9 m below the surface and exhibits Cr(VI) concentrations ranging from 2.5 to 4 mg/L. The injection rate was set to a constant value of 1 mL/min and the amount of injected molasses was controlled by its concentration in the injected aqueous solution. By analogy to the column experiments, a molasses concentration of 200 mg/L in the aquifer was targeted initially. The concentration of molasses was then progressively increased over the course of the experiment until it reached a peak concentration of 3200 mg/L in the aquifer between June 20 and July 25, 2018. Subsequently, the concentration was reduced to 1600 mg/L because the molasses accumulated excessively in the injection well. The molasses concentration in the injected solution needed to reach the target concentration in the aquifer was estimated using the parameters shown in Table 2. Because all parameters except those describing the well geometry are spatially and/or seasonally variable, the targeted molasses concentrations (Table 2) should be considered to be rough estimates.

The wells used to monitor the field experiment were chosen according to the results of a multi-tracer experiment performed in 2010.[19] Based on the identified fast hydraulic connection with the Cr(VI) hotspot, well KB2/13 (15 m downstream from the injection, Fig. 1) was initially considered as the main monitoring well. Thus, it was continuously monitored for oxygen and temperature and sampled weekly for chemical analysis. Starting on August 6, 2018, weekly sampling and analysis were also conducted at well KB1/5. In addition, intermittent sampling and analysis were performed at KB8/3, and KB7/25 (Fig. 1). Potassium was considered to be a conservative tracer owing to its high concentration in the purchased stock molasses

(3.7 wt. %, Table 1) and was used to monitor the possible breakthrough of the injected molasses in all monitoring wells.

Table 2: Field parameters used to determine the molasses concentration in the injection well and corresponding injection protocol

Parameter	**Value**
Porosity	0.23
Groundwater velocity	12 m/day
Darcy velocity	2.76 m/day
Screen length KB6/17	1.75 m
Diameter KB6/17	11 cm
Groundwater flux through the screen	531 L/day
Dilution factor between KB6/17 and KB2/13	3
Injection period	**Target molasses concentrations**
May 30 – June 6, 2018	200 mg/L
June 6 – June 15, 2018	400 mg/L
June 15 – June 20, 2018	600 mg/L
June 20 – July 25, 2018	3,200 mg/L
July 25 – Sept. 29, 2018	1,600 mg/L

Analytical methods. *Column experiments*. Sampling of the column experiments was performed bi-weekly through effluent tubes connected to the top of the columns. The *pH* values were immediately determined upon sampling with a Thermo Scientific Orion 3-Star Benchtop *pH* meter. Samples were stored at 4 °C for less than 2 weeks until performing Cr(VI) and Fe(II) analyses by UV-Vis spectrophotometry (Shimadzu UV-2501PC) using 1,5-diphenylcarbazide (DPC) and ferrozine solutions, respectively. The storage time before analysis was due to logistical constraints. Owing the low storage temperature, it is assumed to have had little effect on the measured Cr(VI) and Fe(II) concentrations, although minor reduction of Cr(VI) to Cr(III) as

well as reactions involving Fe(II) after sample collection cannot be completely excluded.

The DPC solution used for Cr(VI) analyses was prepared with 62.5 mg of DPC powder (Acros Organics, sym-Diphenylcarbazide, 98%, ACS reagent) and 25 mL of acetone (Acros Organics, Acetone, 99.6%, ACS reagent). The samples were processed in 2 mL tubes away from direct light using 675 μL of 0.12 M H_2SO_4, 150 μL of unacidified sample or standard, and 375 μL of DPC solution. The sample was vortexed and transferred to 1.5 mL cuvettes, and the absorbance measured at 540 nm. The relative error, based on multiple measurements of standard samples, is ± 5%, with a detection limit of 10 μg/L. Blank measurements showed that the accuracy was not impacted by the presence of highly diluted molasses such as at the targeted concentration of 200 mg/L. However, owing to minor Cr(VI) reduction potentially occurring after sample storage, the relative error may be slightly larger for concentrations below 100 μg/L.

Samples for Fe(II) analysis by the ferrozine method[23] were acidified upon collection with 0.5 M HCl at a 1:1 sample to acid ratio. The ferrozine solution was prepared using 0.0985 g of Ferrozine powder (Acros Organics, Ferrozine iron reagent, hydrate, 98+%), 1.1915 g of HEPES and 100 mL of milli-Q water. The solution was set to *pH* 7 with a 1 M NaOH solution. The samples were processed in 1.5 mL cuvettes using 100 μL of acidified sample or standard, and 900 μL of ferrozine solution. The absorbance was then measured at 562 nm, with an uncertainty of ± 1 μg/L and a detection limit of 1 μg/L. If Fe(II) did remain reactive during sample storage as described above, however, the effective detection limit and the measurement uncertainty for our column experiment samples may be slightly higher.

Field experiment. All field samples were collected with an Eijkelkamp peristaltic pump at a depth of 6 m and after 15 minutes of pre-pumping at about 2 L/min. Subsequently, the samples were stored at 4 °C until analysis. Samples foreseen for total Cr and K, as well as cations analyses were acidified on-site with 2 drops of a 30% HNO_3 solution after filtration at 0.45 μm. Prior to sampling, the water table was measured with an Ott water level contact gauge. Dissolved organic carbon (DOC) concentrations were measured in filtered, unacidified samples with an Analytic Jena multi NC 2100s TOC analyzer. Alkalinity titration was done with a Metrohm Titrino DMP 785 instrument using a 0.02 M HCl titration solution. The relative standard error is ± 5%.

Total K and Cr concentrations were determined with Inductively Coupled Plasma Optical Emission Spectroscopy (ICP-OES, Agilent Varian ICP-OES 700 ES), with a relative error of ± 5% and a detection limit of 5 μg/L for total Cr. Major cations (Na^+, Ca^{2+}, Mg^{2+}) and anions (Cl^-, SO_4^{2-}, NO_3^-) were measured by ion chromatography (IC) (Metrohm ProflC AnCat MCS and Metrohm IC Compact 861) with a relative standard error of ± 5%. Cr(VI) concentrations were determined on-site with a Merck portable colorimetric kit (MColortest 1.14402.0001). Because the Cr(VI) concentration of the majority of the samples from KB2/13 and KB6/17 was above the upper detection limit of the kit, the samples were diluted with deionized water prior to the measurement, which lowered its accuracy. For undiluted samples, the uncertainty is ± 5 μg/L. For diluted samples, the uncertainty is up to ± 20%.

Oxygen monitoring at KB2/13 was performed continuously using a portable HQ30D multimeter combined with a Hach LDO101 optical dissolved oxygen (DO) probe installed at a depth of 5 m for the duration of the experiment. The multimeter recorded the *in situ* dissolved O_2 concentration, O_2 saturation and temperature at 30

min intervals during 4 consecutive days each week. The same multimeter and probe were used for weekly measurements in KB1/5 and KB6/17, as well as intermittent measurements in KB8/3 and KB7/25. Intermittent *pH* measurements were performed on-site using a Knick Portamess-913 field equipment.

Cr isotope analysis. A selection of samples from both experiments was analyzed for total dissolved Cr (Cr(III) & Cr(VI)) stable isotopes. About 200 ng of Cr were used per analysis for each sample, previously acidified to pH 2 with 30% HCl. A ^{50}Cr - ^{54}Cr double spike[24,25] was added to the samples in a Teflon beaker with a Cr_{sample} to $Cr_{double\text{-}spike}$ ratio of 1:1. The spiked samples were dried completely on a hot plate at 120 °C, then redissolved with 5 mL of 1 M HNO_3, before 110 µL of 30% H_2O_2 (Romil UpA) was added to each beaker. The solutions were left for at least 5 days to ensure complete dissolution, sample-spike equilibration and conversion to Cr(III).[26]

Chromatographic separation of Cr was done in cation columns filled with a 1 mL resin bed (Bio-Rad Ag, 50W-X8 Resin, 200-400 mesh), following a method adapted from Yamakawa et al.[27] and described in detail by Rickli et al.[24] All acids used were sub-boiling distilled. One sample with a very high molasses content (27.6 g/L DOC) was processed with an additional oxidation step prior to carrying out cation exchange chromatography, in order to remove the organic compounds. The sample was refluxed twice overnight, once with 0.5 mL of concentrated HNO_3, once with 1 mL 1 M HNO_3 and 1 mL 30% H_2O_2. The sample was dried between each step.

To measure the Cr isotopic ratio, the purified Cr samples were dissolved in 1 mL 0.5 M HNO_3, transferred to 2 mL acid-cleaned tubes and adjusted with 0.5 M HNO_3 to yield approximately 100 ppb sample Cr. The samples were measured on a Neptune MC-ICP-MS using an Aridus II desolvating system (Cetac) and a Savillex nebulizer

with a nominal uptake rate of 100 μL/min. The instrument performance was tested prior to the sample analyses by measuring at least 6 unspiked NIST 979 standards and three NIST 979 - double spike mixtures.[24] Cr stable isotope data are presented as the derivation of the $^{53}Cr/^{52}Cr$ ratio of the sample from the reference standard NIST SRM 979 in delta notation in ‰ (Eq. 1) with 2 SEM error. Values were corrected for the daily mean NIST SRM 979 $\delta^{53}Cr$, determined from at least 12 measurements.[24] The external reproducibility, based on repeated analysis of a 100 ppb spiked NIST 979 solution over the course of this study, is ±0.023 ‰ (2 SD, n = 42), which is comparable to or smaller than the analytical uncertainty on individual sample measurements.

$$\delta^{53}Cr = \left(\frac{^{53}Cr/^{52}Cr_{sample}}{^{53}Cr/^{52}Cr_{standard}} - 1 \right) \cdot 1000 \quad (1)$$

RESULTS

Column experiment. In the first column, the molasses injection ran smoothly during approximately 35 days (Fig. 2A). After two weeks, dark precipitates that may represent biofilms started appearing around the sediments (see Fig. S3, Supporting Information). After day 36, frequent leakage was observed in the line and a porosity decrease was deduced from increased leaking at the base of the column. After day 59, the column was completely clogged, likely due to excessive biofilm production, and the peristaltic pump was no longer able to maintain a constant flux through the column. As a consequence, the column was disconnected and left in the same oxic and temperature controlled room (20 °C) for 70 days in order to allow the biomass to degrade sufficiently before resuming the experiment. On day 130, the column was reconnected and the experiment ran smoothly until day 150 (Fig. 2A).

From the beginning of the molasses injection, the effluent Cr(VI) concentration decreased rapidly. After a short increase between days 26 and 33 due to clogging of the influent molasses tubes (presumably caused by microbial growth), no Cr(VI) could be detected in the effluent until the column was completely clogged on day 59. During the second injection phase, starting on day 130, the Cr(VI) concentration dropped immediately and was not detectable after two weeks (i.e., on day 144). The drop in the Cr(VI) concentration to undetectable levels was 25% faster during the second injection phase. Fe(II) was detected occasionally in the first injection phase, with a maximal concentration of 8 μg/L that was measured when Cr(VI) was almost completely reduced. A rust-colored precipitate was visible in the transparent effluent tubes after one week of injection (see Fig. S3, Supporting Information). Rust patches were also visible inside the column, around the sediments.

In the second column, the injection of molasses ran smoothly during 43 days (Fig. 2B). Dark precipitates likely representing biofilms developed around the sediments in the first week of the experiment. The Cr(VI) concentration sharply decreased after the start of the molasses injection. Cr(VI) was not detected in the effluent between days 16 and 21 as well as between days 35 and 43. After day 43, tube leakage and disconnection occurred frequently and could not be mitigated. Fe(II) was not detected in the effluent of the second column, however, as in the first column, a rust-colored precipitate developed in the effluent tubes and around the sediment grains. In both columns, the *pH* in the effluent was between 7.5 and 8.0 and hence slightly lower than in the injected groundwater, where the *pH* value was around 8.0.

Five column effluent samples were measured for Cr isotopes. The obtained δ^{53}Cr values ranged from 0.58‰ to 1.83‰, and hence showed variations well above the measurement uncertainty (Fig. 3; Tables S1-S2, Supporting Information). In contrast,

the injected Cr(VI)-bearing groundwater showed quasi-constant δ^{53}Cr values, between 0.63‰ and 0.72‰. High δ^{53}Cr values correlate with a low remaining Cr(VI) fraction *f* in the effluent and all data follow a Rayleigh distillation model (Fig. 3),

$$\delta^{53}Cr = \left((\delta^{53}Cr_{initial} + 1000) \cdot f^{(\alpha-1)}\right) - 1000 \qquad (2)$$

where $\delta^{53}Cr_{initial}$ refers to the average δ^{53}Cr value of the injected groundwater (0.68‰) and α refers to the effective isotopic fractionation factor. Alpha was calculated from the slope of the best-fit line from the linearized Rayleigh plot ln(δ^{53}Cr +1000‰) versus ln(*f*),[28] resulting in a value of 0.99875, which corresponds to an enrichment factor ε of -1.25 ‰. The observed ε is well within the ε-range of -0.4 to -4.4 determined for other Cr(VI) reduction experiments (see compilation by Wanner and Sonnenthal[29]).

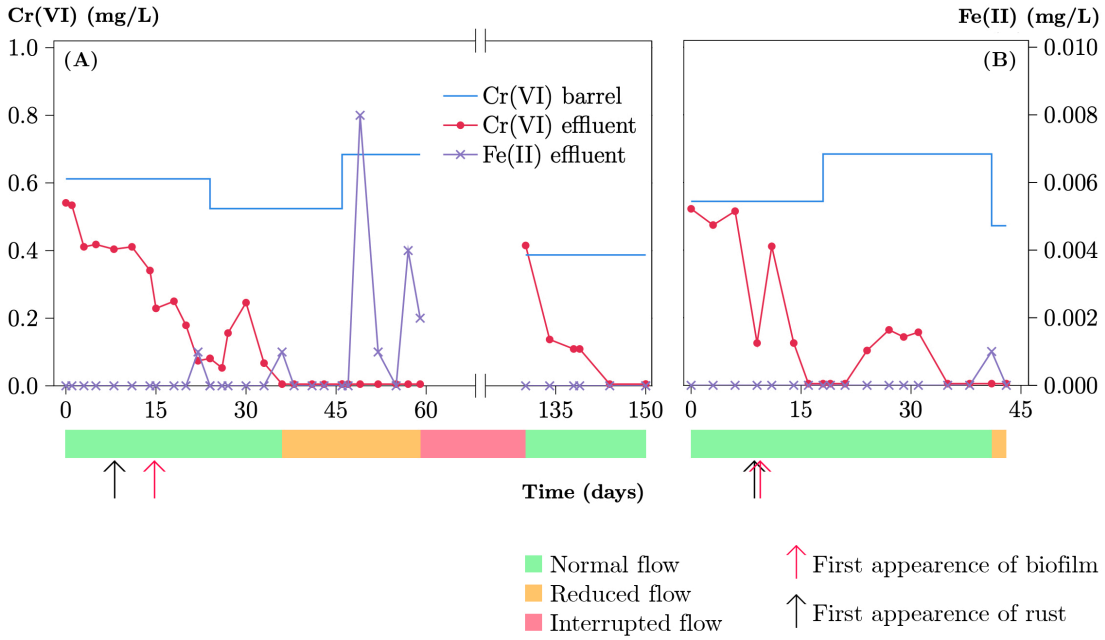

Figure 2. Evolution of the Cr(VI) and Fe(II) concentrations in the column experiment and Cr(VI) concentration in the injected groundwater. Left graph: Column no. 1. Right graph: Column no. 2. The colored bar codes illustrate the different flow conditions observed during the experiments, and the arrows mark the onset of biofilm and rust formation,

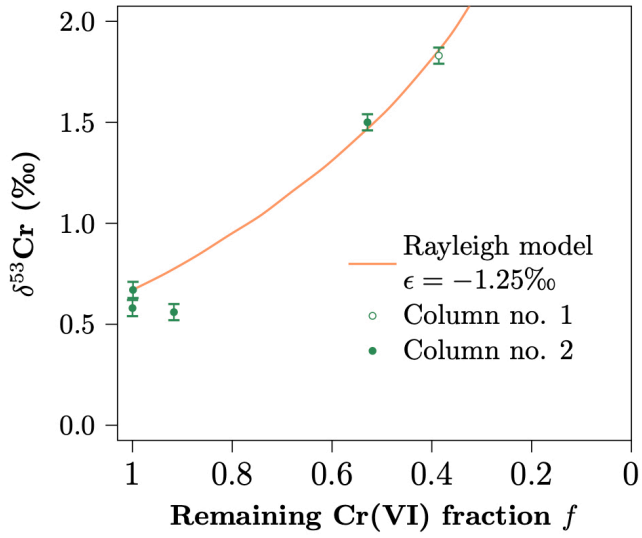

Figure 3. Cr isotope data for the column experiment.

Field experiment. The biogeochemical response of the aquifer to the injection of molasses showed strong spatial and temporal variations. This is described below in detail for the injection well and each of the monitoring wells (Fig. 1). The raw data are provided in Tables S3-S7 (Supporting Information).

Injection well KB6/17. In the first two months of injection (June-July 2018), the DO concentration in the KB6/17 injection well (Fig. 1) decreased from 10 to 4 mg/L. In August 2018, roughly two months after the start of the injection, the well became fully anoxic and Cr(VI) concentrations decreased below 0.5 mg/L (Fig. 4A). Between August 6 and October 4, 2018, the groundwater in KB6/17 was a dark brown color (Fig. 4B) that persisted even after pre-pumping over 100 L. For this reason, Cr(VI) could not be measured during this period (as it relies on a colorimetric assay). Simultaneously, concentrations of DOC and K increased dramatically, while the *pH* dropped to 4.3 (Fig. 4C). Moreover, a frothy layer developed on the surface of the

water inside the well during this period. In contrast to Cr(VI), the concentrations of total Cr did not decrease in early August, when anoxic conditions were established, but remained roughly at the 2.5 mg/L background level measured prior to the injection of molasses (Fig. 4A). A representative chemical analysis for the peak anoxic conditions observed in August-September 2018 is provided in Table 3.After stopping the injection at the end of September 2018, the color of the samples became clear within 5 days. Simultaneously, the DOC concentration immediately dropped to values below 30 mg/L, before gradually decreasing to the background concentration (<1 mg/L) in January 2019 (Fig. 4A). Along with DOC, the total Cr concentration dropped immediately below 0.5 mg/L when the injection was stopped. Very low Cr(VI) concentrations (0.005-0.5 mg/L) as well as anoxic conditions prevailed until the end of January 2019 (Fig. 4C), four months after having stopped the delivery of molasses.

Monitoring for Cr isotopes showed $\delta^{53}Cr$ variations well above the measurement uncertainty (Fig. 4D). The first two samples collected in April and July 2018 yielded similar $\delta^{53}Cr$ values of 0.69 and 0.64 ‰. These values agree well with measurements performed in 2010 and 2011[19] and hence correspond to the background isotopic composition of this particular hotspot domain. In the later stages of the experiment, a shift of $\delta^{53}Cr$ first towards lower (0.24 ‰, September 2018) and then towards higher values (1.44 ‰, December 2018) was observed.

Table 3: Full chemical analyses of groundwater samples collected in KB6/17 on April 4 (background conditions) and September 13 (peak anoxic conditions) 2018, as well as selected results from geochemical modeling.

	April 4, 2018	**Sept 13, 2018**	**[2]Source**
pH	7.33	4.3	Fermentation
O_2 saturation %	87	< 5	Microbial activity
Cr total (mg/L)	2.54	2.19	Cr(VI) hotspot
Na (mg/L)	1.82	920	Molasses
K (mg/L)	0.71	3485	Molasses
Ca (mg/L)	47.5	129	Calcite
Mg (mg/L)	5.18	5.54	Groundwater
Fe (mg/L)	<0.01	7.31	Fe-sulfides
S total (mg/L)	12.4	312	Fe-sulfides
δ^{53}Cr (‰)	0.63	0.24	
DIC (mg/L)	25	106.6	Calcite, molasses
DOC (mg/L)	0.64	27,580	Molasses
[1]Mackinawite saturation index	n.a.	-1.23	n.a.
[1]pH at mackinawite saturation	n.a.	5.21	n.a

[1]PHREEQC calculations (Wateq4f database) assuming that 2/3 of total sulfur is dissolved as sulfide species.
[2]Possible sources for the increased concentration observed in the September 13 sample

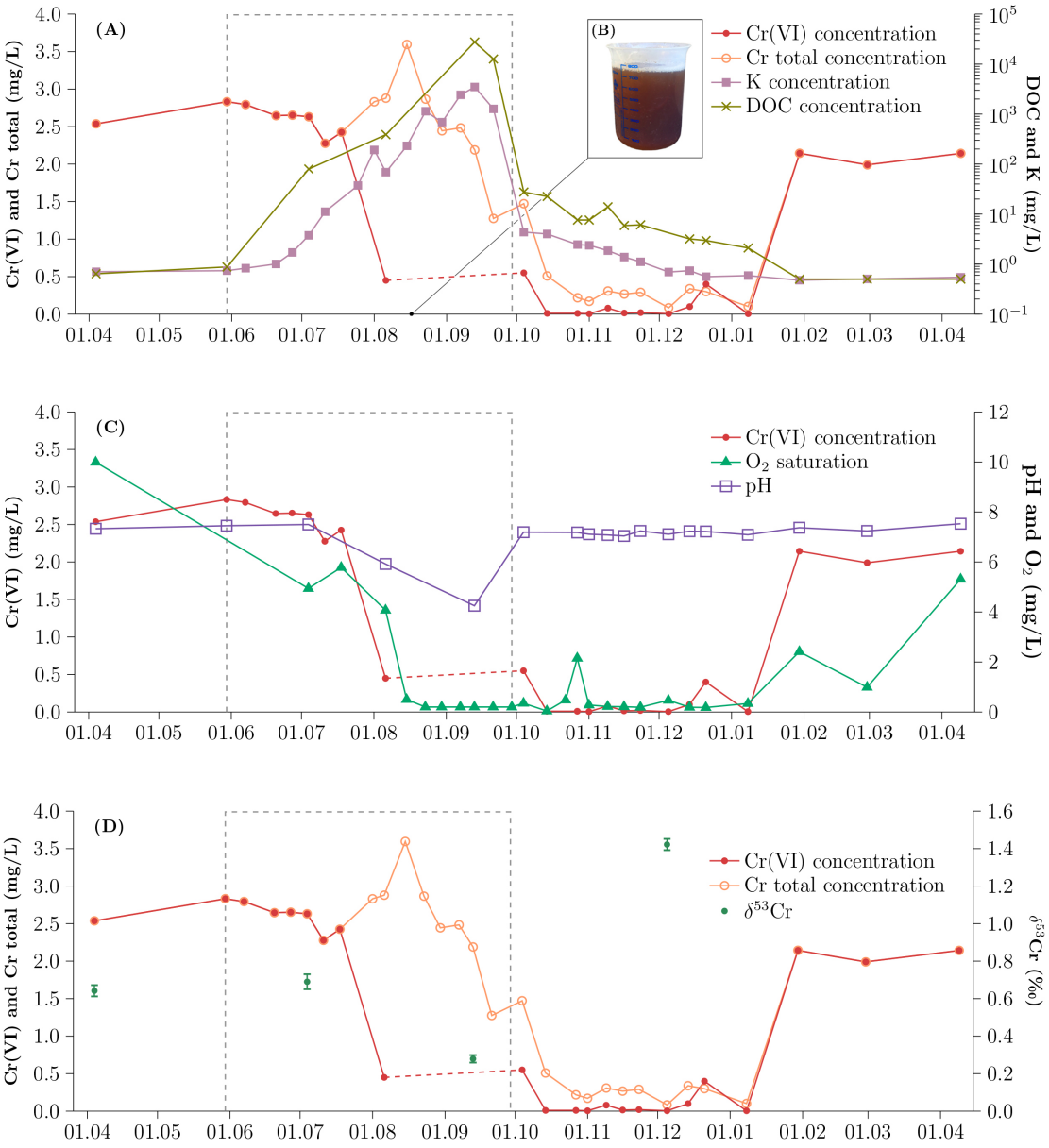

Figure 4. Monitoring results for KB6/17 between April 2018 and April 2019. The dashed line represents the molasses injection period. (A) DOC, K, Cr(VI) and total Cr concentrations. The dashed section of the chromate curve corresponds to the period during which the samples were too opaque to be measured. (B) Photograph showing the accumulation of molasses in the water in August-September 2018. (C) DO concentration, pH and Cr(VI) concentration. (D) δ^{53}Cr values, Cr total and Cr(VI) concentrations.

Monitoring wells KB2/13, KB8/3, and KB7/25. The continuous monitoring of KB2/13 (Fig. 1) for DO concentration and temperature showed important seasonal variations (Fig. 5A). The groundwater temperature ranged from 6.3 °C in early April 2018 to 21.1 °C in August 2018 before gradually decreasing to values below 7 °C in February 2019. As expected, the DO concentration was inversely proportional to the groundwater temperature, with a maximum of 11.5 mg/L in February 2019 and a minimum below 6 mg/L between July and September 2018. Thus, oxidizing conditions prevailed at this monitoring well during the entire course of the field experiment, although a notable decrease of the O_2 saturation from 90 to 70% was observed in July and August 2018. The groundwater table level rose from 4.2 m below the surface in April 2018 to 3.2 m in early June 2018, before progressively falling again to 4.2 m at the end of October 2018 (Fig. 5B). The initial groundwater table rise was accompanied by a decrease of the Cr(VI) concentration from about 1.5 mg/L in April and May 2018 to values below 0.8 mg/L for the reminder of the experiment (Fig. 5B). Neither the DOC nor the K concentrations observed in KB2/13 displayed any significant change during the injection period (Fig. 5B). $\delta^{53}Cr$ values measured for KB2/13 range from 0.63‰ to 0.72‰ and hence showed no significant variation (Fig. 5C).

The intermittent sampling and analyses of KB8/3 and KB7/25 (Fig. 1) yielded nearly constant K concentrations and O_2 saturations, while the Cr(VI) concentration showed minor variations (Tables S6 and S7, Supporting Information).

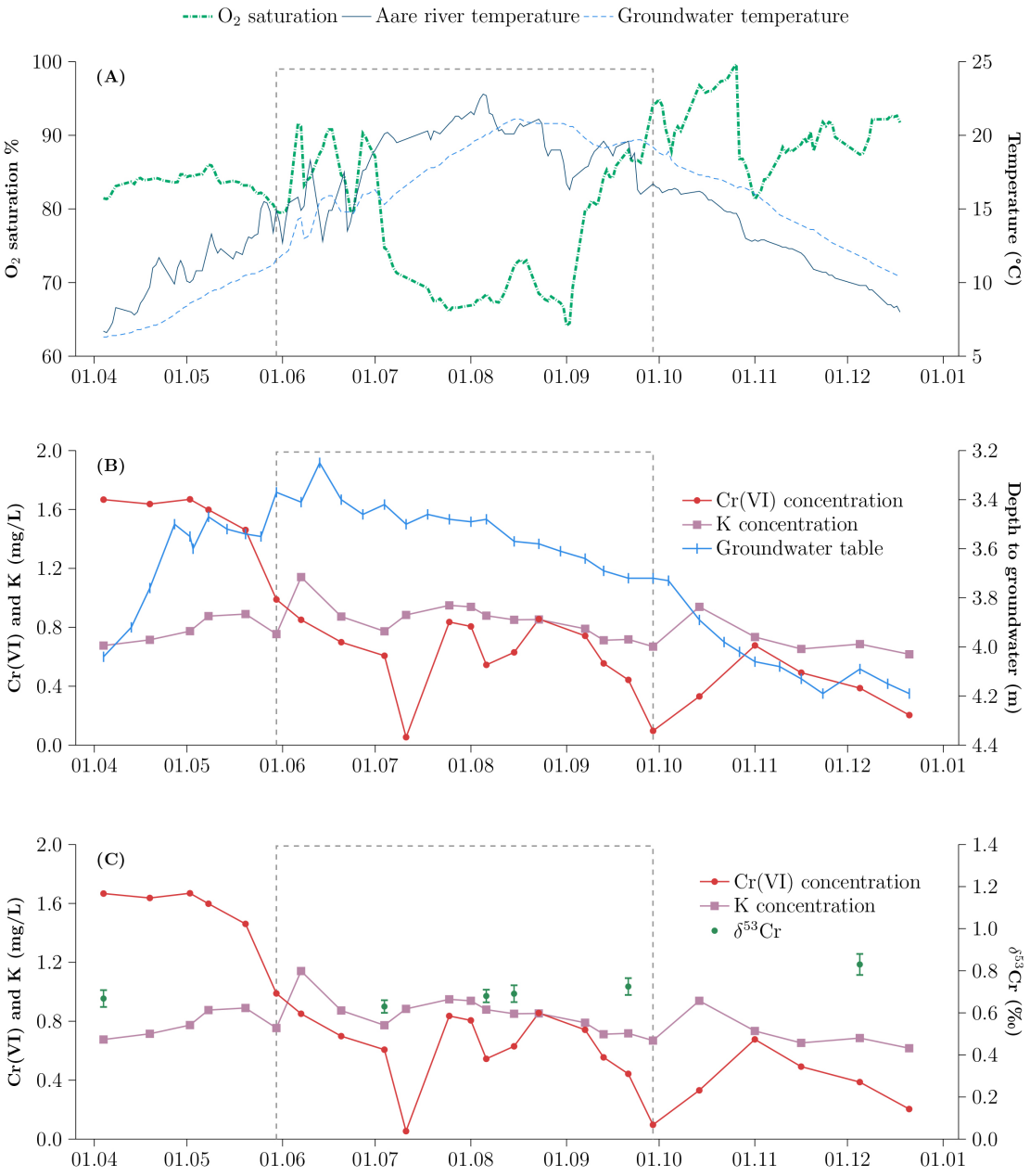

Figure 5. Monitoring results for KB2/13 from April to December 2018. The dashed line represents the molasses injection period. (A) O_2 saturation and temperature of the groundwater, temperature of the Aare river continuously recorded by the Swiss Federal Office for the Environment 400 m downstream from the study site. (B) Groundwater table depth, Cr(VI) and K concentrations. (C) $\delta^{53}Cr$ values, K and Cr(VI) concentrations.

Monitoring well KB1/5. During the peak anoxic conditions observed in August-September 2018 in the injection well (Fig. 4), a strong response was observed in monitoring well KB1/5 despite its large distance (170 m) from the injection point (Fig. 1). In the second week of August 2018, the K concentration increased from 1.2 to 2.3 mg/L, while the O_2 saturation and Cr(VI) concentration decreased to values below 40% and 10 μg/L, respectively (Figs. 6A, B). Subsequently, similar values prevailed until the injection was stopped at the end of September 2018. Afterwards, the K concentration progressively decreased to almost constant concentrations around 0.6 mg/L in mid-October. Simultaneously, the O_2 saturation progressively increased until reaching 80% in December 2018. Along with O_2, the concentration of Cr(VI) continuously increased, until reaching a maximum of 13 μg/L in early November 2018.

In terms of Cr isotopes, δ^{53}Cr values showed important variations (0.64 to 1.14‰) and tended to decrease simultaneously with the Cr(VI) concentration (Fig. 6C). However, the measured δ^{53}Cr values are within the range reported for the isotopically heterogeneous hotspot (0.62 to 1.38‰).[19]

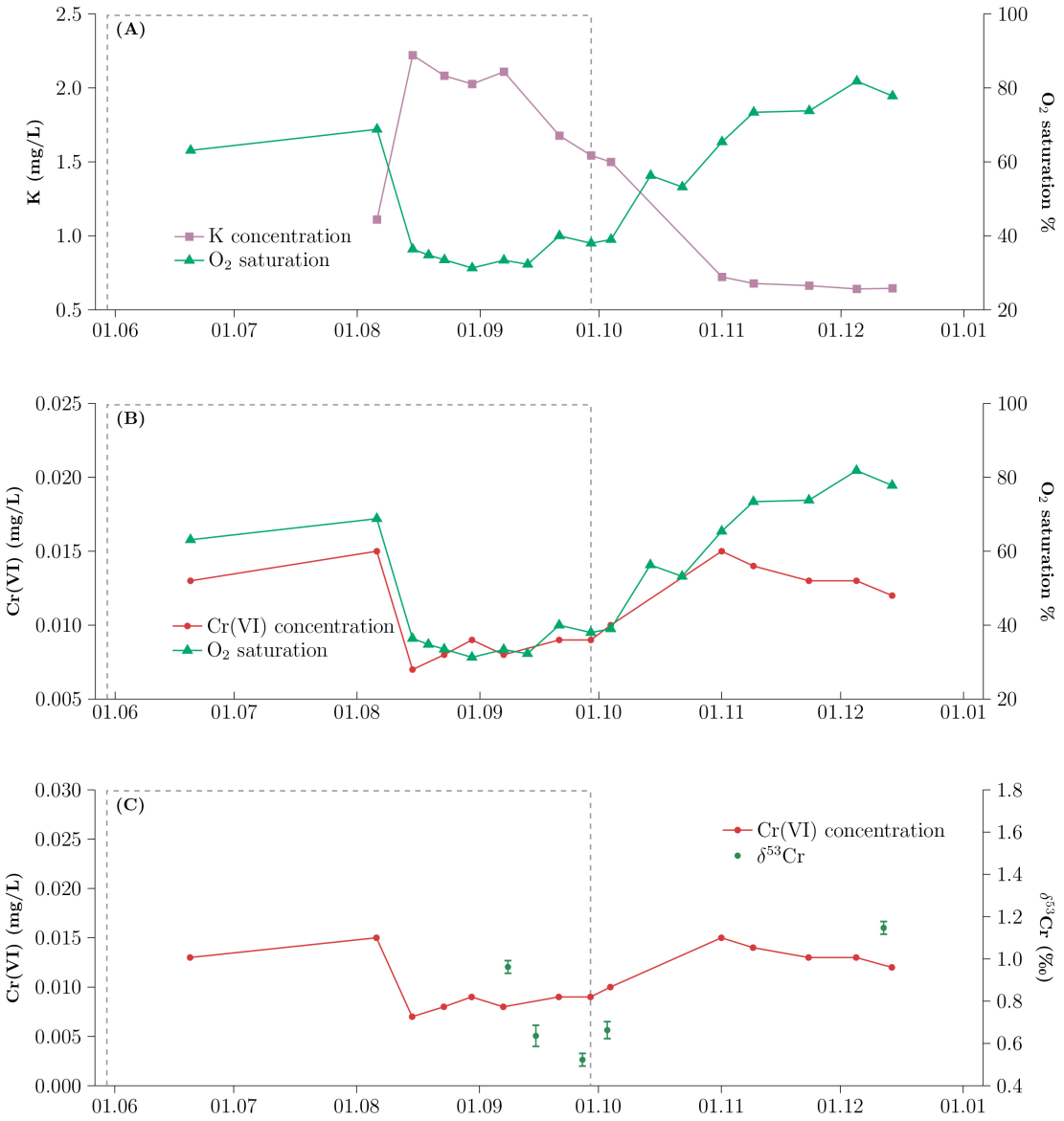

Figure 6. Monitoring results for KB1/5 between June and December 2018. The dashed line represents the injection period. (A) O_2 saturation and K concentration. (B) O_2 saturation and Cr(VI) concentration. (C) $\delta^{53}Cr$ values and Cr(VI) concentrations.

DISCUSSION

Results from both the column and field experiments provided multiple lines of evidence that microbiologically-mediated Cr(VI) reduction can be successfully achieved by injecting molasses into aquifers characterized by oxygen-saturated conditions and groundwater flow velocities above 10 m/day. The most important

observation was that column effluents were at least temporarily Cr(VI) free (Fig. 2) and that anoxic conditions with very low Cr(VI) concentrations were achieved in the injection well during the field experiment (Fig 4). The simultaneous occurrence of the Cr(VI) concentration and O_2 saturation minima, as well the concurrent breakthrough of the molasses tracer (i.e. [K]) in monitoring well KB1/5 (Fig. 6), further confirmed that Cr(VI) reduction was successfully stimulated in the field experiment. Finally, as Cr(VI) reduction is the only known process that can lead to significant Cr isotope fractionation[18], it was further confirmed by the Cr isotopic fractionation observed in the column experiments (Fig. 3) and in the injection well of the field experiment (Fig. 4D).

The rust patches observed in the column experiments (Fig. S3, Supporting Information) confirmed the presence of mobile Fe(II) in the columns (rapidly oxidized to Fe(III) upon contact with O_2), suggesting that metabolic Fe(II) inherited from microbial Fe(III) reduction was likely involved in Cr(VI) reduction, either exclusively or in combination with microbial Cr(VI) reduction.[9]

The time lag of 1–2 months until anoxic and low Cr(VI) conditions were established in the column and field experiments (Figs. 2, 4) indicates that the microbial community must become sufficiently established to alter the redox conditions and permit Cr(VI) reduction. A similar time lag was reported in a previous Cr(VI) bioremediation experiment.[5] In our field experiment, the delay was further controlled by seasonal temperature variations, as microbial growth rates increase with temperature,[30] and the temperature of the groundwater increased from 10 °C to 20 °C during the injection period (Fig. 5A).

Beside showing that microbiologically-mediated Cr(VI) reduction can be successfully stimulated under high flow rates and oxic conditions, our experiments

allowed us to identify several challenges that have to be met for a site-scale implementation aiming at treating entire groundwater Cr(VI) plumes. These challenges are summarized in the conceptual model provided in Fig. 7 and are individually described below.

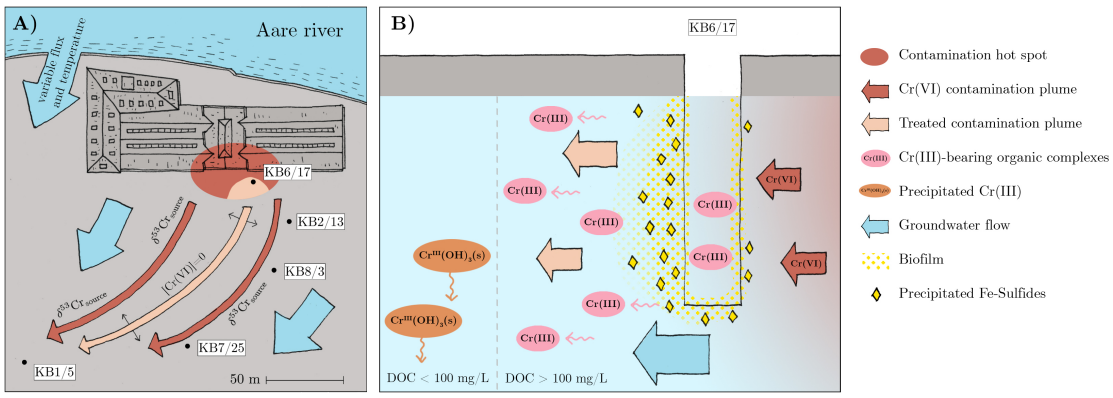

Figure 7. Conceptual model illustrating the main challenges for a site-scale implementation. (A) Map view of the site showing that narrow preferential flow paths control the dispersion of the injected molasses and hence the extent where the Cr(VI) plume was treated successfully. Dispersive mixing of the different flow paths does not result in detectable Cr isotope fractionation. The proximity to the Aare river leads to strong variations in temperature as well in the degree of dilution of the Cr(VI) plume. (B) Vertical profile of the injection well showing that the porosity may be decreased by excessive biofilm formation and precipitation of Fe-sulfides. At DOC concentrations above 100 mg/L, Cr(III) may remain in solution.

Injectivity decrease. The dark brown color of the groundwater pumped from the injection well during peak anoxic conditions in August-September 2018 (Fig. 4B) is inherited from the accumulation of molasses in the well. The molasses accumulation suggests that the porosity and hence the well injectivity decreased during injection. The decrease most likely results from excessive biofilm formation in and around the well (Fig. 7B). The presence of a large microbial community is further confirmed by

the low *pH* of 4.3 (Fig. 4B) resulting from the fermentation of the accumulated molasses and the subsequent formation of CO_2 and low molecular organic acids such as lactic and acetic acids. While in case of the column experiments, biofilm formation led to complete clogging and subsequent interruption of the experiments (Fig. 2), during the field experiment the delivery of molasses into the aquifer had persisted despite the reduced injectivity. This is inferred from the observation that the color of injection well samples became clear within 5 days after stopping the injection at the end of September 2018.

In addition to biofilm formation, the injectivity decrease observed in the field experiment may have been caused by the formation of Fe-sulfides (Fig. 7B), as inferred from very high Fe and S concentrations measured in the injection well during peak anoxic conditions (Table 3). Geochemical modeling performed using PHREEQC[31] suggests that high Fe and S concentrations are inherited from the dissolution of previously precipitated Fe-sulfides, such as mackinawite (FeS). Supersaturated mackinawite may have first precipitated at *pH* levels above 5.2 (Table 3), as a consequence of microbial sulfide reduction occurring during peak anoxic conditions. Subsequently, as the *pH* dropped to values as low as 4.3, mackinawite became strongly undersaturated (Table 3) and thus prone to dissolution.

Avoiding excessive biofilm formation and clogging of the injection well represents an important challenge for the successful distribution of molasses into the aquifer, because it may influence the groundwater flow paths around the injection well, similar to the unwanted consequences of the PRB implementation in 2008.[19] Nevertheless, limited biofilm formation is desirable because it increases the resilience of the bacterial community[32,33] necessary to mediate chromate reduction.

Complexation of Cr(III) with organic ligands. The distinct evolutions of Cr(VI) and total Cr in the KB6/17 injection well (Fig. 4) are due to the presence of Cr(III) in solution together with Cr(VI) (Fig. 7B). The presence of Cr(III) in solution is attributed to the complexation of Cr(III) by organic ligands as a consequence of high DOC concentrations (up to 27.58 g/L), which prevents its removal by co-precipitation with Fe-hydroxides.[34,35] Moreover, at the low *pH* of 4.3 observed during the accumulation of molasses (Fig. 4C), the *Eh-pH* conditions were close to the Cr^{3+} stability field[36] and therefore allowed for the presence of Cr(III) in solution without extensive formation of dissolved organic Cr(III) species. In any case, the increased mobility of Cr(III) is an unwanted feature caused directly or indirectly by the presence of large amounts of molasses in the vicinity of the injection well. The simultaneous decrease of the concentrations of DOC and total Cr observed in the post-injection period (Fig. 4A) demonstrate that the mobility of Cr(III) concentrations strongly decreases when the DOC concentration drops to about 100 mg/L (Fig. 7B).

Preferential flow paths. Elevated K concentrations (i.e. molasses tracer, Table 1) were measured in KB1/5 but in none of the other monitoring wells. This indicates that the injected molasses was transported along very narrow preferential flow paths and only reached KB1/5 (Fig. 7A). A direct hydraulic connection between the injection well and KB1/5 is consistent with a tracer experiment carried out in 2020,[19] and the long distance between the two wells (170 m) suggest that the preferential flow paths are particularly strong. Preferential flow paths are due to small-scale heterogeneities and a strong exchange between groundwater and surface water, as it is typical for alluvial gravel aquifers.[37] Since preferential flow paths control the distribution of the

injected molasses, their occurrence represent an important challenge for the homogenous distribution of molasses across the entire Cr(VI) plume.

Seasonal hydrogeological variations. At our study site, the Aare river (Fig. 1) exerts a strong control over the hydrogeochemical conditions of the aquifer as manifested by the O_2 saturation recorded in the monitoring well closest to the river (KB2/13, Fig. 1). For instance, the drop in oxygen saturation observed in July 2018 (Fig. 5) resulted from a positive temperature gradient of up to 5 °C between the nearby Aare river and the aquifer (Fig. 5A). Thus, oxygen-saturated river water infiltrating into the aquifer during the hot summer months cools down significantly. As a consequence, the O_2 saturation decreases to around 70% along the flow path even if the O_2 concentration remains constant. At the end of August 2018, the temperature gradient was reversed and the Aare temperature was up to 4 °C below the groundwater temperature, causing a warming up of the infiltrating river water and a subsequent increase of the O_2 saturation to around 90% (Fig. 5A). The direct hydraulic connection between the Aare river and KB2/13 may also have a distinct effect on the Cr(VI) concentration. In April and May 2018 the river and groundwater table increased by about 1 m which resulted in the concurrent decrease of the Cr(VI) concentration from 1.5 to 0.8 mg/L (Fig. 5B) due to increased dilution of the Cr(VI) plume by river water infiltrating into the aquifer. Owing to the temperature-dependence of microbial growth rates[30] and their potential limitation by elevatated Cr(VI) concentrations, the strong seasonal variations in groundwater temperature and Cr(VI) concentrations caused by the proximity to the Aare river (Fig. 7a) form an important boundary condition for planning future stimulation measures.

The use Cr isotopes to track Cr(VI) reduction during biostimulation in alluvial aquifers. Even though Cr(VI) reduction is clearly associated with Cr isotope fractionation, as observed in the column experiments (Fig. 3), the use of Cr isotopes to track Cr(VI) reduction during field-scale injection of molasses is not straightforward. In our field experiment, quantitative Cr(VI) reduction occurred in and around the injection well (Fig. 4C). Under such conditions, samples from downstream wells typically represent a mixture of at least two distinctive flow paths, one with quantitative Cr(VI) reduction, where fractionation cannot be observed because the reduction is complete, and one without reduction, and therefore no fractionation (Fig. 7a). This resulted in changes to Cr(VI) concentrations due to reduction that was not reflected in δ^{53}Cr values.

The likely presence of dissolved, isotopically light Cr(III) in solution along with isotopically heavy Cr(VI) represented an additional challenge in the tracking of Cr(VI) reduction. In the injection well, for instance, the presence of soluble Cr(III) likely caused the δ^{53}Cr shift towards both lower and higher values (Fig. 4D). The negative shift observed in September 2018 can be explained by a mixed Cr pool consisting of (i) isotopically light Cr(III), either instantaneously produced from Cr(VI) reduction or resulting from the dissolution of previously precipitated Cr(III) due to the low *pH* of 4.3 (Table 3), and (ii) isotopically heavy Cr(VI). Similarly, the December sample may correspond to a mixture of Cr(VI) and Cr(III), albeit with a lower Cr(III) concentration and a greater reductive removal of Cr(VI), which resulted in lower total dissolved Cr and Cr(VI) concentrations and a net positive δ^{53}Cr shift (Fig. 4D).

A third challenge occurs when the Cr(VI) source is isotopically heterogeneous. In our field experiment, the concentration evolutions of DO, Cr(VI) and K provided

strong evidence that Cr(VI) reduction was successfully stimulated at monitoring well KB1/5. Nevertheless, the decrease in Cr(VI) concentration was accompanied by an inconsistent shift of $\delta^{53}Cr$ towards lower values (Fig. 6). This negative $\delta^{53}Cr$ shift likely resulted from variations in the flow field and therefore of the hydraulic connection between KB1/5 and different parts of the isotopically heterogeneous hotspot ($\delta^{53}Cr$ values from 0.62 to 1.38‰[19]) that were unaffected by Cr(VI) reduction.

In order to gain a better understanding of such complex systems and to allow for more informed interpretations of Cr isotope analyses aiming to track treated Cr(VI) plumes, additional studies performing compound-specific Cr isotope analyses (i.e. separate isotope analyses for Cr(VI) and Cr(III)) are needed.

Persistence and extent of the induced redox shift. The persistence of the induced reducing conditions is a key parameter for a site-scale stimulation of microbially-mediated Cr(VI) reduction. In our field experiment, anoxic and low Cr(VI) conditions prevailed for four months after the injection of molasses was stopped while the DOC concentrations dramatically decreased (Fig. 4). This implies that relatively low DOC concentrations of less than 10 mg/L are sufficient to maintain an active microbial community capable of mediating Cr(VI) reduction. Moreover, it confirms that microbial communities are persistent[32,33] even in the presence of high flow rates and cold winter temperatures below 10 °C. This is consistent with an experiment conducted at Hanford, USA, were the injection of electron donors (hydrogen release compound) led to an increase of biomass concentrations as well as a redox potential decrease that lasted for at least 3 years.[5]

Although the long-term local establishment of reducing conditions can mitigate the Cr(VI) pollution, its overall environmental impact can be negative if the reducing

conditions extend beyond the Cr(VI) contamination plume and pose the risk of reducing the aquifer on a regional scale. Such was the case in a similar hydrogeological setting, where the improper disposal of sugar-derived waste products led to the durable establishment of reducing conditions that lasted at least several decades[38] and were accompanied by high concentrations of ammonium, as well as dissolved Mn(II) and Fe(II), that precluded the use of the entire aquifer as a water resource.

Based on our experiments, a repeated injection of limited amounts of molasses appears to be a promising solution for meeting both challenges, i.e., achieving a long-term stimulation of Cr(VI) reduction while avoiding the unwanted reduction of the uncontaminated portion of the aquifer. As observed in the first column experiment (Fig. 2A), repeated injections could decrease the time needed to initiate Cr(VI) reduction. Moreover, owing to the persistent nature of microbes,[32,33] the period with prevailing reducing conditions after the end of the injection may increase with each injection cycle. Considering the high groundwater flow rate and the high dilution factor, it is reasonable to expect that the targeted injection of small amounts of molasses will not affect large portions of the aquifer. Nevertheless, regular monitoring is necessary.

CONCLUSIONS

Column and field experiments convincingly demonstrate that microbiologically-mediated Cr(VI) reduction can be successfully achieved by injecting molasses into aquifers characterized by oxygen-saturated conditions and high groundwater flow rates. The main challenges encountered during the field experiment include a substantial injectivity decrease attributed to the formation of biofilm and Fe-sulfides,

and the heterogeneous distribution of molasses due to the presence of narrow preferential flow paths. Several implications for large-scale electron donor injections as a remediation measure for Cr(VI) contaminated sites with similar conditions have been identified:

- The injection should be performed from several points evenly positioned in and around the contamination hotspot to promote the dispersion of the electron donor across the entire Cr(VI) plume by making use of the preferential flow paths.
- The concentration of the injected electron donor in the aquifer should be optimized to avoid excessive growth, while promoting adequate reductive immobilization of Cr(VI). Limiting the electron donor concentration will likely prevent the dispersion of Cr(III) by dissolution or complexation with organic ligands. Based on our field experiment, a DOC concentration of 10 mg/L is sufficient to induce significant microbiologically-mediated Cr(VI) reduction if molasses is chosen as the electron donor.
- Injection should be performed during summer time, to take advantage of the higher temperatures favorable to bacterial growth. Moreover, owing to the decreased solubility of oxygen with increasing temperature, anoxic conditions are more readily attainable during the summer months.
- Multiple injections performed during consecutive summers are most promising because they may favor the formation of a robust microbial community and reduce the activation time at the beginning of each injection period. Ideally, this could result in persistent reducing conditions resulting in long-term Cr(VI) reduction. If persistent reducing conditions cannot be

achieved, the development of an optimal site-specific injection protocol may still represent a cost-effective and sustainable remediation strategy.

ACKNOWLEDGMENTS

The field experiment was funded by the "Amt für Wasser und Abfall des Kantons Bern". Franz Schenker is acknowledged for fruitful discussion. Practical support during the field experiment by Tom Schwarz and Zlatko Perica from the Konzepthalle 6 is greatly appreciated. EPFL funding for hosting Dan Alessi in summer 2018 is also acknowledged. Chromium isotope data were obtained on a Neptune MC-ICP-MS acquired with funds from the NCCR PlanetS supported by SNSF grant 51NF40-141881. Comments of two anonymous reviewers helped to improve the manuscript and are highly acknowledged.

ASSOCIATED CONTENT

Photographs of the experimental setups and additional data tables are provided as Supporting Information (PDF).

REFERENCES

1. Apte, A. D.; Tare, V.; Bose, P., Extent of oxidation of Cr(III) to Cr(VI) under various conditions pertaining to natural environment. *J. Hazard. Mater.* **2006,** *128* (2-3), 164-174.

2. Rai, D.; Sass, B. M.; Moore, D. A., Chromium(III) hydrolysis constants and solubility of chromium(III) hydroxide. *Inorg. Chem.* **1987,** *26* (3), 345-349.

3. Kanojia, R. K.; Junaid, M.; Murthy, R. C., Embryo and fetotoxicity of hexavalent chromium: a long-term study. *Toxicol. Let.* **1998,** *95* (3), 165-172.

4. Kotas, J.; Stasicka, Z., Chromium occurrence in the environment and methods of its speciation. *Environ. Pollut.* **2000,** *107* (3), 263-283.

5. Faybishenko, B.; Hazen, T. C.; Long, P. E.; Brodie, E. L.; Conrad, M. E.; Hubbard, S. S.; Christensen, J. N.; Joyner, D.; Borglin, S. E.; Chakraborty, R.; Williams, K. H.; Peterson, J. E.; Chen, J.; Brown, S. T.; Tokunaga, T. K.; Wan, J.; Firestone, M.; Newcomer, D. R.; Resch, C. T.; Cantrell, K. J.; Willett, A.; Koenigsberg, S., In Situ long-term reductive bioimmobilization of Cr(VI) in groundwater using Hydrogen Release Compound. *Environ. Sci. Technol.* **2008,** *42* (22), 8478-8485.

6. Varadharajan, C.; Beller, H. R.; Bill, M.; Brodie, E. L.; Conrad, M. E.; Han, R.; Irwin, C.; Larsen, J. T.; Lim, H.-C.; Molins, S.; Steefel, C. I.; van Hise, A.; Yang, L.; Nico, P. S., Reoxidation of chromium(III) products formed under different biogeochemical regimes. *Environ. Sci. Technol.* **2017,** *51* (9), 4918-4927.

7. Jeyasingh, J.; Somasundaram, V.; Philip, L.; Bhallamudi, S. M., Pilot scale studies on the remediation of chromium contaminated aquifer using bio-barrier and reactive zone technologies. *Chem. Eng. J.* **2011,** *167* (1), 206-214.

8. Tebo, B. M.; Obraztsova, A. Y., Sulfate-reducing bacterium grows with Cr(VI), U(VI), Mn(IV), and Fe(III) as electron acceptors. *FEMS Microbiol. Lett.* **1998,** *162* (1), 193-198.

9. Zhang, Q.; Amor, K.; Galer, S. J. G.; Thompson, I.; Porcelli, D., Using stable isotope fractionation factors to identify Cr(VI) reduction pathways: Metal-mineral-microbe interactions. *Water Res*. **2019,** *151*, 98-109.

10. Fendorf, S.; Wielinga, B. W.; Hansel, C. M., Chromium Transformations in Natural Environments: The role of biological and abiological processes in chromium(VI) reduction. *Int. Geol. Rev*. **2000,** *42* (8), 691-701.

11. Beller, H. R.; Yang, L.; Varadharajan, C.; Han, R.; Lim, H. C.; Karaoz, U.; Molins, S.; Marcus, M. A.; Brodie, E. L.; Steefel, C. I.; Nico, P. S., Divergent aquifer biogeochemical systems converge on similar and unexpected Cr(VI) reduction products. *Environ. Sci. Technol*. **2014,** *48* (18), 10699-10706.

12. Suthersan, S. S., Engineered in situ anaerobic reactive zones. *United States Patent 6,143,177. Nov. 7. 2000* **2000**.

13. Jamieson-Hanes, J. H.; Gibson, B. D.; Lindsay, M. B. J.; Kim, Y.; Ptacek, C. J.; Blowes, D. W., Chromium isotope fractionation during reduction of Cr(VI) under saturated flow conditions. *Environ. Sci. Technol*. **2012,** *46* (12), 6783-6789.

14. Bill, M.; Conrad, M. E.; Faybishenko, B.; Larsen, J. T.; Geller, J. T.; Borglin, S. E.; Beller, H. R., Use of carbon stable isotopes to monitor biostimulation and electron donor fate in chromium-contaminated groundwater. *Chemosphere* **2019,** *235*, 440-446.

15. Michailides, M. K.; Tekerlekopoulou, A. G.; Akratos, C. S.; Coles, S.; Pavlou, S.; Vayenas, D. V., Molasses as an efficient low-cost carbon source for biological Cr(VI) removal. *J. Hazard. Mater*. **2015,** *281*, 95-105.

16. Salunkhe, P. B.; Dhakephalkar, P. K.; Paknikar, K. M., Bioremediation of hexavalent chromium in soil microcosms. *Biotechnol. Lett.* **1998,** *20* (8), 749-751.

17. Schmieman, E. A.; Yonge, D. R.; Rege, M. A.; Petersen, J. N.; Turick, C. E.; Johnstone, D. L.; Apel, W. A., Comparative kinetics of bacterial reduction of chromium. *J. Environ. Eng.* **1998,** *124* (5), 449-455.

18. Ellis, A. S.; Johnson, T. M.; Bullen, T. D., Chromium isotopes and the fate of hexavalent chromium in the environment. *Science* **2002,** *295* (5562), 2060-2062.

19. Wanner, C.; Zink, S.; Eggenberger, U.; Mäder, U., Unraveling the partial failure of a permeable reactive barrier using a multi-tracer experiment and Cr isotope measurements. *Appl. Geochem.* **2013,** *37*, 125-133.

20. Qin, L.; Wang, X., Chromium isotope geochemistry. *Rev. Mineral. Geochem.* **2017,** *82*, 379–414.

21. Wanner, C.; Zink, S.; Eggenberger, U.; Mäder, U., Assessing the Cr(VI) reduction efficiency of a permeable reactive barrier using Cr isotope measurements and 2D reactive transport modeling. *J. Cotam. Hydrol.* **2012,** *131*, 54-63.

22. Alessi, D. S.; Wang, Y.; Falquet, L.; Gay-des-Combes, J.; Cordier, D.; Bernier-Latmani, R., Products of microbial Cr(VI) reduction in biostimulated alluvial aquifer sediments. *Abstract to the 2013 GSA Annual Meeting in Denver* **2013**.

23. Stookey, L. L., Ferrozine---a new spectrophotometric reagent for iron. *Anal. Chem.* **1970,** *42* (7), 779-781.

24. Rickli, J.; Janssen, D. J.; Hassler, C.; Ellwood, M. J.; Jaccard, S. L., Chromium biogeochemistry and stable isotope distribution in the Southern Ocean. *Geochim. Cosmochim. Acta* **2019,** *262*, 188-206.

25. Rudge, J. F.; Reynolds, B. C.; Bourdon, B., The double spike toolbox. *Chem. Geol.* **2009,** *265* (3), 420-431.

26. Larsen, K. K.; Wielandt, D.; Schiller, M.; Bizzarro, M., Chromatographic speciation of Cr(III)-species, inter-species equilibrium isotope fractionation and improved chemical purification strategies for high-precision isotope analysis. *J. Chromatogr. A* **2016,** *1443*, 162-174.

27. Yamakawa, A.; Yamashita, K.; Makishima, A.; Nakamura, E., Chemical separation and mass spectrometry of Cr, Fe, Ni, Zn, and Cu in terrestrial and extraterrestrial materials using thermal ionization mass spectrometry. *Anal. Chem.* **2009,** *81* (23), 9787-9794.

28. Scott, K. M.; Lu, X.; Cavanaugh, C. M.; Liu, J. S., Optimal methods for estimating kinetic isotope effects from different forms of the Rayleigh distillation equation. *Geochim. Cosmochim. Acta* **2004,** *68* (3), 433-442.

29. Wanner, C.; Sonnenthal, E. L., Assessing the control on the effective kinetic Cr isotope fractionation factor: A reactive transport modeling approach. *Chem. Geol.* **2013,** *337*, 88-98.

30. Ratkowsky, D. A.; Olley, J.; McMeekin, T. A.; Ball, A., Relationship between temperature and growth rate of bacterial cultures. *J. Bacteriol.* **1982,** *149* (1), 1.

31. Parkhurst, D. L.; Appelo, C. A. J., Description of input and examples for PHREEQC version 3—A computer program for speciation, batch-reaction, one-

dimensional transport, and inverse geochemical calculations. *U.S. Geological Survey Techniques and Methods* **2013,** *book 6, chap. A43*, 497 p, available only at http://pubs.usgs.gov/tm/06/a43.

32. Costerton, J. W.; Lewandowski, Z.; Caldwell, D. E.; Korber, D. R.; Lappin-Scott, H. M., Microbial Biofilms. *Annu. Rev. of Microbiol.* **1995,** *49* (1), 711-745.

33. O'Toole, G.; Kaplan, H. B.; Kolter, R., Biofilm formation as microbial development. *Annu. Rev. Microbiol.* **2000,** *54* (1), 49-79.

34. James, B. R.; Bartlett, R. J., Behavior of Chromium in Soils: V. Fate of organically complexed Cr(III) added to soil. *J. Environ. Qual.* **1983,** *12* (2), 169-172.

35. Nakayama, E.; Kuwamoto, T.; Tokoro, H.; Fujinaga, T., Chemical Speciation of Chromium in Sea-Water: Part 1. Effect of naturally occurring organic materials on the complex formation of chromium(III). *Anal. Chim. Acta* **1981,** *130*, 289-294

36. Ball, J. W.; Nordstrom, D. K., Critical evaluation and selection of standard state thermodynamic properties for chromium metal and its aqueous ions, hydrolysis species, oxides, and hydroxides. *J. of Chem. Eng. Data* **1998,** *43* (6), 895-918.

37. Huggenberger, P.; Hoehn, E.; Beschta, R.; Woessner, W., Abiotic aspects of channels and floodplains in riparian ecology. *Freshwater Biol.* **1998,** *40* (3), 407-425.

38. Wersin, P.; Abrecht, J.; Höhener, P., Large-scale redox plume in glaciofluvial deposits due to sugar-factory wastes and wastewater at Aarberg, Switzerland. *Hydrogeol. J.* **2001,** *9* (3), 282-296.

For Table of Contents Only